Supplementary Table 1. List of antibodies

Antibody	Host	Application	Catalog number	Vendor
anti-HSP90	Mouse	WB	sc-13119	Santa Cruz Biotechnology
anti-α-tubulin	Mouse	WB	T5168	Sigma-Aldrich
anti-PRMT1	Rabbit	WB	07-404	EMD Millipore
Total OXPHOS Rodent WB	Mouse	WB	ab110413	Abcam
anti-AKT	Rabbit	WB	#9272	Cell Signaling Technology
anti-p-AKT (S473)	Rabbit	WB	#9271	Cell Signaling Technology
anti-FOXO1	Rabbit	WB	#9454	Cell Signaling Technology
anti-FOXO3a	Rabbit	WB	#12829	Cell Signaling Technology
anti-PRMT6	Rabbit	WB	#14641	Cell Signaling Technology
anti-LC3A/B	Rabbit	WB	#4108	Cell Signaling Technology
Autophagy sampler kit	Rabbit	WB	#4445	Cell Signaling Technology
anti-AMPKα	Rabbit	WB	#2532	Cell Signaling Technology
anti-p-AMPKα (T172)	Rabbit	WB	#2535	Cell Signaling Technology
anti-HSL	Rabbit	WB	#4107	Cell Signaling Technology
anti-p-HSL (S660)	Rabbit	WB	#4126	Cell Signaling Technology
anti-UCP1	Rabbit	WB	ab10983	Abcam
ANTI-FLAG® M2-Peroxidase (HRP) antibody	Mouse	WB	A8592	Sigma-Aldrich
PE anti-mouse CD140a Antibody	Rat	Cell isolation	135905	BioLegend
Anti-PE MicroBeads	Mouse	Cell isolation	130-048-801	Miltenyi Biotec
anti-Pyruvate Dehydrogenase	Mouse	IF	ab110333	Abcam
anti-F4/80	Rat	IHC	ab6640	Abcam

anti-LC3B	Mouse	IF	#83506	Cell Signaling Technology
anti-Perilipin-1	Rabbit	IF	#9349	Cell Signaling Technology
Alexa Fluor® 568 Goat Anti-Rabbit (IgG) secondary antibody	Goat	IF	A11011	Invitrogen
Alexa Fluor® 488 Goat Anti-Mouse (IgG) secondary antibody	Goat	IF	A11001	Invitrogen
anti-rat IgG-HRP	Goat	IF	sc-2006	Santa Cruz Biotechnology
Anti-FOXO3a	Rabbit	ChIP	#2497	Cell Signaling Technology

Supplementary Fig. Legends.

Supplementary Fig. 1. Adipocyte-specific depletion of *Prmt1* eliminates expression of *Prmt1* in mature adipocytes.
A. *Prmt1* mRNA levels in mature adipocytes (M.A) and stromal vascular fraction (SVF) from 2-month-old C57BL/6 mice with NCD (n=4 and n=5, respectively). Relative mRNA expression was normalized to *L32* expression. **B.** Western blot analysis showing PRMT1 protein levels from various adipose tissues as well as the liver and the skeletal muscle from *Prmt1* f/f and FKO mice (n=3/group). **C.** Western blot analysis showing PRMT1 protein levels in mature adipocytes from eWAT and iWAT. Representative blot from three independent experiments was shown. Data in **A** represent mean ± SEM. ***; $P < 0.001$.

Supplementary Fig. 2. Depletion of *Prmt1* does not affect glucose and lipid metabolism under normal chow diet conditions.
A-C. Body weight (**A**), organ weight (as a percentage of body weight) (**B**), and fat and lean mass (**C**) in 4- month-old *Prmt1* f/f and FKO mice fed normal chow diet (NCD) were shown (n=6-8/group). **D-F.** *Ad libitum* fed (**D**), 6 hr fasted (**E**), and overnight fasted (O/N, 16 hr) (**F**) blood glucose levels from 4-month-old *Prmt1* f/f and FKO mice under NCD (n=6-8/group). **G** and **H.** Plasma non-esterified fatty acids levels (**G**) and plasma triglyceride levels (**H**) in 6 hr-fasted 4-month-old *Prmt1* f/f and FKO mice under NCD (n=5-6/group). **I.** Insulin tolerance test (ITT) of 4-month-old *Prmt1* f/f and FKO mice under NCD. ITT was conducted after the intraperitoneal injection of insulin (0.5 units/kg) on 6 hr-fasted mice (n=6-8/group). Data in **A-I** represent mean ± SEM. *; $P < 0.05$, **; $P < 0.01$.

Supplementary Fig. 3. Adipocyte specific *Prmt1* KO mice shows reduced eWAT.
A-G. Representative images showing eWAT (**A**), iWAT (**B**), rpWAT (**C**), pWAT (**D**), BAT (**E**), Skeletal muscle (**F**), and Liver (**G**) from *Prmt1* f/f and FKO mice fed HFD for 16 weeks. (**H**) Body weight, fat, and lean mass of *Prmt1* f/f and FKO mice fed HFD for 10 weeks (n=8-13/group). Data in **H** represent mean ± SEM.

Supplementary Fig. 4. Adipocyte-specific *Prmt1* KO mice did not greatly affect adipocyte size in iWAT.
A. Representative images of hematoxylin and eosin-stained sections from iWAT depots of *Prmt1* f/f and FKO mice with 12 weeks of high-fat feeding. Scale bar = 250 μm. **B.** Quantification of number and size of adipocytes from iWAT of *Prmt1* f/f and FKO mice with 12 weeks of high-fat feeding. Data in **B** represent mean ± SEM.

Supplementary Fig. 5. *Prmt1* deficiency does not greatly affect lipolysis.
A. Relative mRNA levels of genes encoding lipases (ATGL, HSL) in eWAT (left) and iWAT (right) from *Prmt1* f/f and FKO mice fed HFD for 12 weeks (n=3-6/group). **B.** Protein levels of HSL and p-HSL in eWAT (left) and iWAT (right) from *Prmt1* f/f and FKO mice fed HFD for 12 weeks (n=6/group). **C.** Released glycerol levels from explants of eWAT (left) and iWAT (right) of *Prmt1* f/f and FKO mice fed HFD for 20 weeks (n=4/group). Lipolysis was stimulated with 10 μM forskolin (Fsk) for 2 hr. Glycerol levels were normalized to tissue weight. Data in **A** and **C** represent mean ± SEM. *; $P < 0.05$, n.s.: not significant.

Supplementary Fig. 6. Depletion of *Prmt1* enhanced expression of AMPK
A. Relative mRNA levels of *Prkaa1 and Prkaa2* in 3T3-L1 adipocytes expressing either the control virus (Ad-US) or shRNA against *Prmt1* (Ad-*Prmt1*i). (n=3/group). mRNA levels were normalized by *L32* expression. **B.** PRMT1, PRMT6, FOXO3, AMPK and p-AMPK levels in 3T3-L1 adipocytes expressing either the control virus (Ad-US) or shRNA against *Prmt1* (Ad-*Prmt1*i). Representative data were shown. **C.** Relative mRNA levels of *Prmt* isoforms in mature adipocytes of eWAT from *Prmt1* f/f and FKO mice fed HFD for 10 weeks (n=3-4/group). **D.** Protein levels of PRMT6 and FOXOs in eWAT from *Prmt1* f/f and FKO mice fed HFD for 16 weeks (n=4-5/group). **E.** Relative mRNA levels of *Prmt1*, *Prmt6*, *Foxo1*, and *Foxo3* in 3T3-L1 adipocytes expressing either the control virus (Ad-US) or shRNA against *Prmt1* (Ad-*Prmt1*i). (n=3/group). mRNA levels were normalized by *L32* expression. **F.** p-AMPKα and AMPKα levels in 3T3-L1 adipocytes with ectopic expression of PRMT6 or FOXO3. Data in **A**, **C**, and **E** represent mean ± SEM. **; $P < 0.01$, ***; $P < 0.001$.

Supplementary Fig. 7. Depletion of *Prmt1* promotes an increased expression of components in the autophagy.
A. Relative mRNA levels of autophagy markers in mature adipocytes of eWAT from *Prmt1* f/f and FKO mice fed HFD for 10 weeks (n=3-4/group). mRNA levels were normalized by *L32*. **B.** Quantitation of proteins involved in the autophagy shown in Fig. 4B. Data in **A** and **B** represent mean ± SEM. *; $P < 0.05$, **; $P < 0.01$, ***; $P < 0.001$.

Supplementary Fig. 8. Depletion of *Prmt1* leads to the enhanced autophagic flux.
A. Quantitation of LC3-II/LC3-I ratio for Fig. 4C (top) and 4D (bottom). **B.** Relative LC3-II levels with injection of lysosomal protease inhibitor leupeptin in Liver (top) or BAT (bottom) of *Prmt1* f/f mice and FKO mice. **C.** Co-localization of LC3B and PLIN1 in iWAT of *Prmt1* f/f mice and FKO mice. Scale bar = 20 μm. **D.** Quantitation of fluorescent intensity to measure co-localization of LC3B and PLIN1 from eWAT (Fig. 4E) and iWAT (Supplementary Fig. 8C). Data in **A** and **D** represent mean ± SEM. *; $P < 0.05$, ***; $P < 0.001$.

Supplementary Fig. 9. *Prmt1* deficiency promotes increased mitochondrial function in adipocytes.
A. Quantitation of the intensity of mitotracker staining in eWAT (Fig. 5B). **B.** Measurement of relative mitochondrial DNA (mtDNA) in eWAT (top) and iWAT (bottom) from *Prmt1* f/f and FKO mice fed HFD for 16 weeks (n=4-5/group). Relative mtDNA was normalized to nuclear DNA (nDNA, *H19*). **C.** Relative mRNA levels of mitochondrial markers in eWAT (left) and iWAT (right) from *Prmt1* f/f and FKO mice after 12 weeks of high-fat feeding (n=3-6/group). mRNA levels were normalized by *L32* expression. Data in **A-C** represent mean ± SEM. *; $P < 0.05$, **; $P < 0.01$, ***; $P < 0.001$.

Supplementary Fig. 10. *Prmt1* deficiency promotes increased mitochondrial function in WAT but not in BAT.
A-D. OxPhos protein levels in rpWAT (**A**), pWAT (**B**), iWAT (**C**) or BAT (**D**) from *Prmt1* f/f and FKO mice after 12 weeks of high-fat feeding (n=5-7/group).

Supplementary Fig. 11. *Prmt1* deficiency promotes increased lipid catabolism via an AMPK pathway.
A. PRMT1, AMPKα, p-AMPK, LC3, and OxPhos protein levels in differentiated 3T3-L1 cells. Cells were transfected with control siRNA, *Prmt1* siRNA, *Prkaa*, or *Prmt1* siRNA + *Prkaa* siRNA before the initiation of differentiation. Representative data from three independent experiments were shown. **B.** PRMT1, AMPKα, p-AMPK, LC3, and OxPhos protein levels in differentiated primary adipocytes (derived from the AP cells of eWAT) from *Prmt1* f/f mice. Cells were transfected with control siRNA, *Prmt1* siRNA, *Prkaa*, or *Prmt1* siRNA + *Prkaa* siRNA before the initiation of differentiation. Representative data from three independent experiments were shown.

Supplementary Fig. 12. *Prmt1* deficiency does not affect the intrinsic lipid catabolism in BAT.
A. Western blot analysis showing UCP1 protein levels in BAT (top) or iWAT (bottom) from *Prmt1* f/f and FKO mice after 12 weeks of high-fat feeding (n=3-6/group). B. Representative images of hematoxylin and eosin-stained sections from BAT depots of *Prmt1* f/f and FKO mice with 12 weeks of HFD feeding under the room temperature (RT) or cold stress. Scale bar = 250 μm.

Supplementary Fig. 13. *Prmt1* deficiency promotes an increased energy expenditure.
A-D. Indirect calorimetric analysis using *Prmt1* f/f and FKO mice with 11 weeks of HFD feeding. Body weight (**A**), Regression-adjusted energy expenditure for body weight (**B**), Regression-adjusted energy expenditure for food intake (**C**), and food intake (**D**) were shown (n=6/group). Data in **A**-**D** represent mean ± SEM. **; $P < 0.01$, ***; $P < 0.001$.

Supplementary Fig. 14. Adipocyte-specific *Prmt1* KO mice promotes adipose tissue inflammation.
A. Representative images of F4/80 immunohistochemistry of eWAT depots (top) or iWAT depots (bottom) from *Prmt1* f/f and FKO mice with 12 weeks of high-fat feeding. Scale bar = 100 μm. **B.** Relative mRNA levels of classic macrophage (M1) and alternative macrophage (M2) markers of eWAT from *Prmt1* f/f and FKO mice fed HFD for 12 weeks (n=4-6/group). mRNA levels were normalized to *L32* expression. **C**. Plasma IL-6 levels and plasma TNFα levels from *Prmt1* f/f and FKO mice with 14 or 12 weeks of high-fat feeding (n=4-6/group). Data in **B** and **C** represent mean ± SEM. *; $P < 0.05$.

Supplementary Fig. 15. Adipocyte-specific *Prmt1* deficiency alters glucose and lipid metabolism.
A. *Ad libitum* fed blood glucose levels from *Prmt1* f/f and FKO mice fed HFD for 9-10 weeks (n=11-12/group). **B.** Plasma insulin levels in 6 hr-fasted of *Prmt1* f/f and FKO mice fed HFD for 14 weeks (n=7-8/group). **C.** Plasma non-esterified fatty acids levels in 6 hr-fasted *Prmt1* f/f and FKO mice fed HFD for 12 weeks (n-5-6/groups). **D.** Relative mRNA levels of genes involved in lipid metabolism in the liver from *Prmt1* f/f and FKO mice fed HFD for 12 weeks (n=5-6/group). Relative mRNA expression was normalized to *L32* expression. **E.** Representative western blot analysis for AKT and p-AKT levels in BAT (left), iWAT (middle) and skeletal muscle (right) from *Prmt1* f/f and FKO mice fed HFD for 10 weeks. Levels of p-AKT (serine 473), total AKT, PRMT1, and loading control (HSP90) in the absence or in the presence of insulin injection were shown. All tissues were collected

from mice post PBS or insulin (0.2 units/mouse) injection. **F**. Quantitation of p-AKT over AKT in BAT (left), iWAT (middle) and skeletal muscle (right) from *Prmt1* f/f and FKO mice fed HFD for 10 weeks (n=3/group). Data in **A**-**D** and **F** represent mean ± SEM. *; $P < 0.05$, **; $P < 0.01$.

Supplementary Fig. 16. Proposed model for PRMT-mediated regulation of lipid homeostasis.
In wild-type mice (left), obesity induces expression of PRMT1, inhibiting excessive lipid catabolism in WAT to prevent unnecessary ectopic accumulation of lipid in the peripheral tissues. In the absence of adipose PRMT1 (right), lipid catabolism in WAT is enhanced via the activation of AMPK and subsequent induction of lipophagy as well as mitochondrial catabolism, leading to the redistribution of lipid in the peripheral tissues and the resultant dysregulation of glucose and lipid homeostasis in the diet-induced obesity setting.

Supplementary Fig. 1

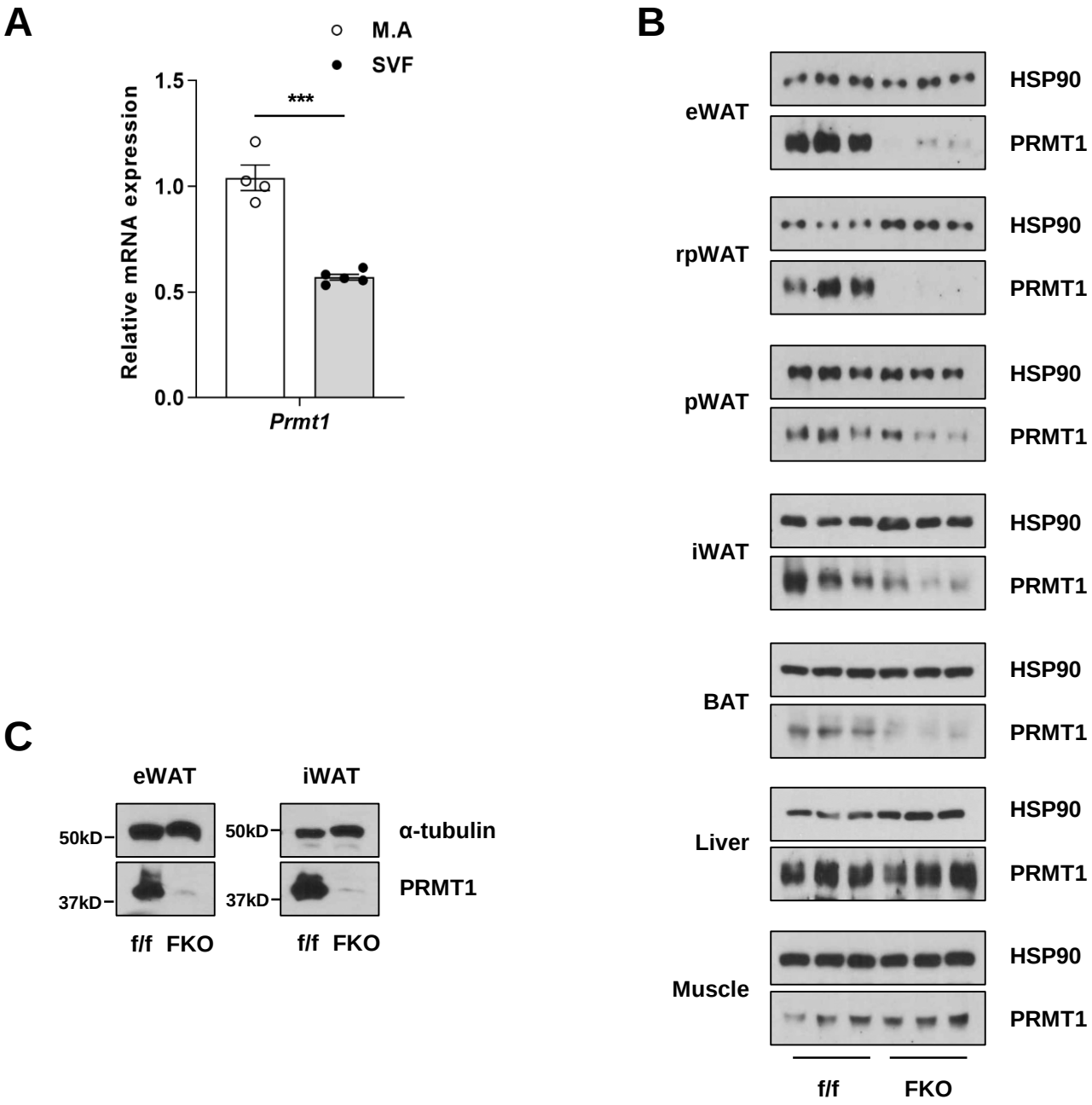

Supplementary Fig. 2

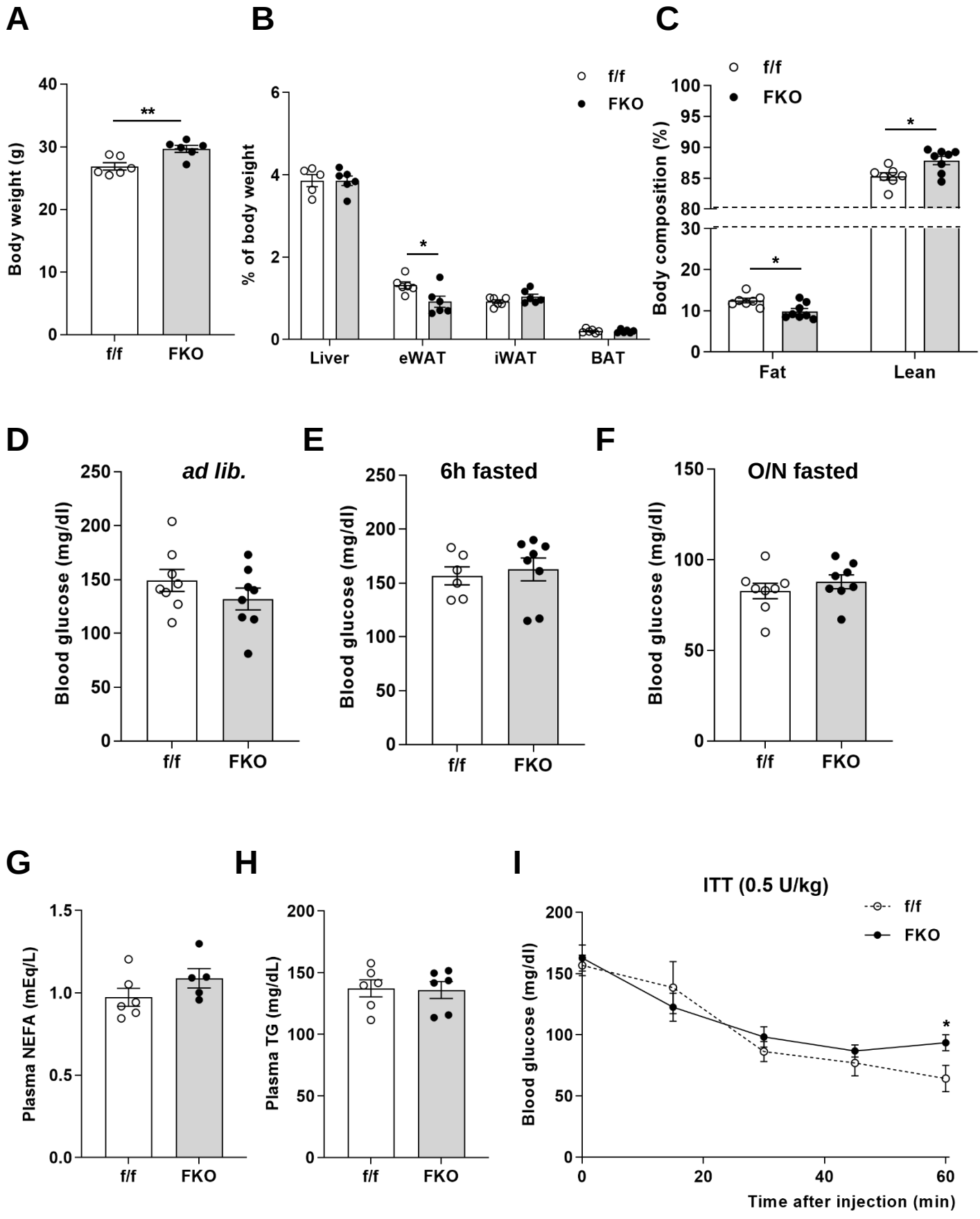

Supplementary Fig. 3

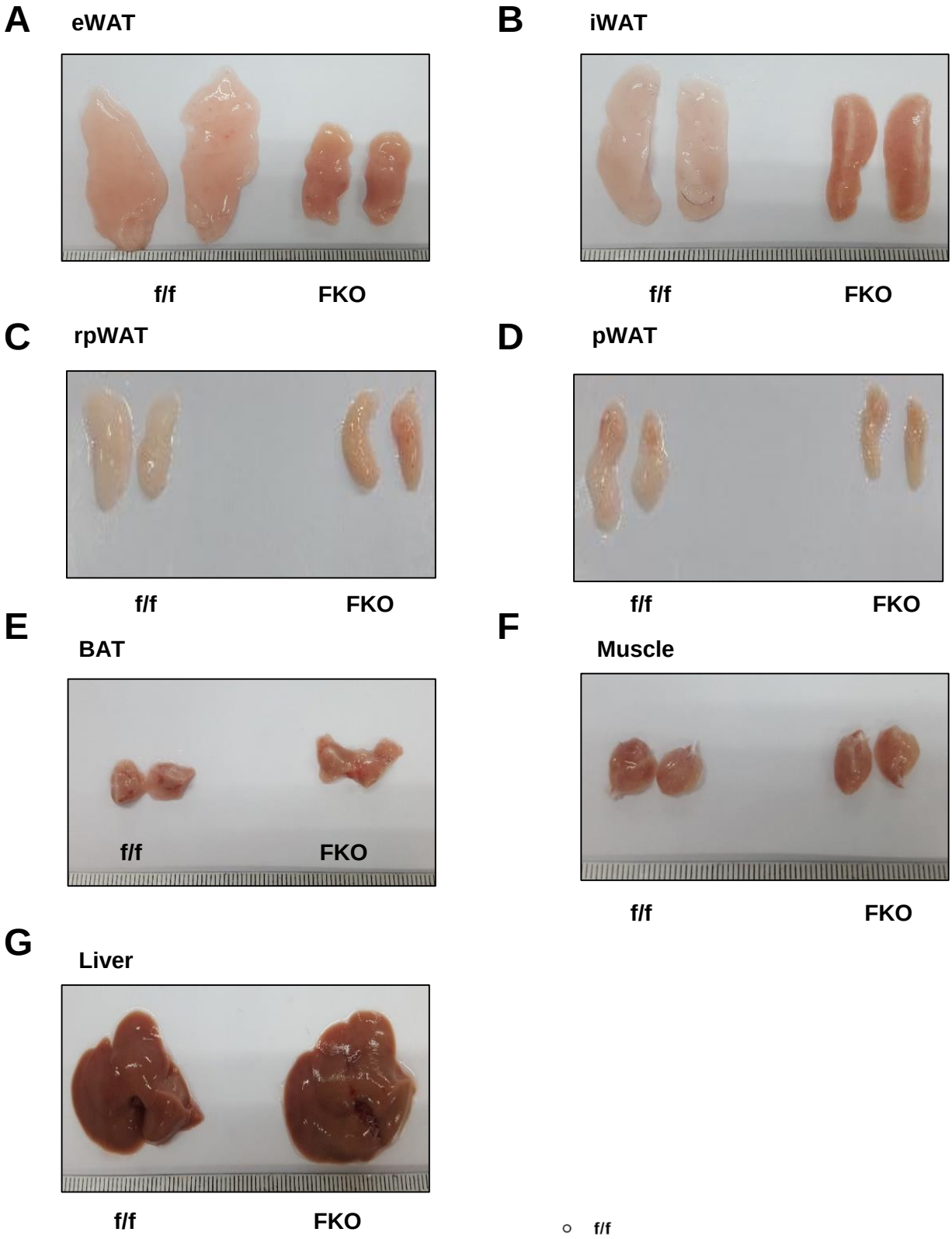

Supplementary Fig. 4

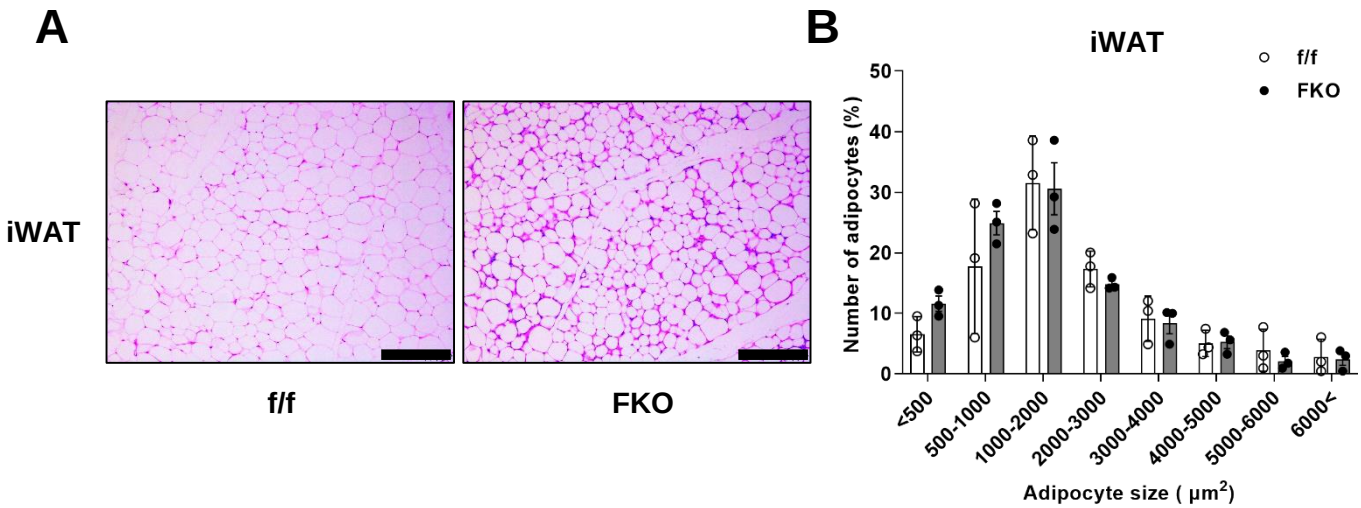

Supplementary Fig. 5

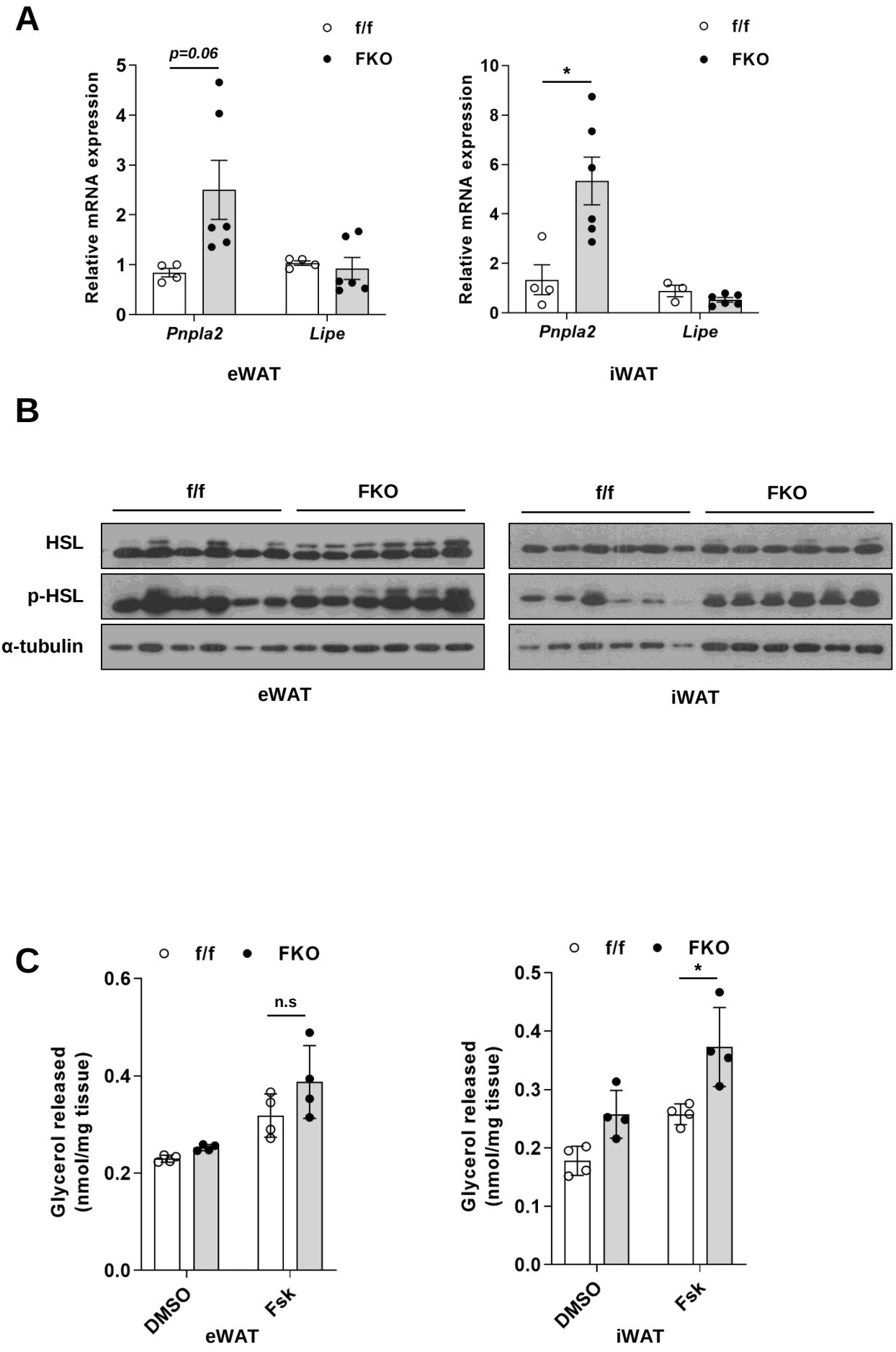

Supplementary Fig. 6

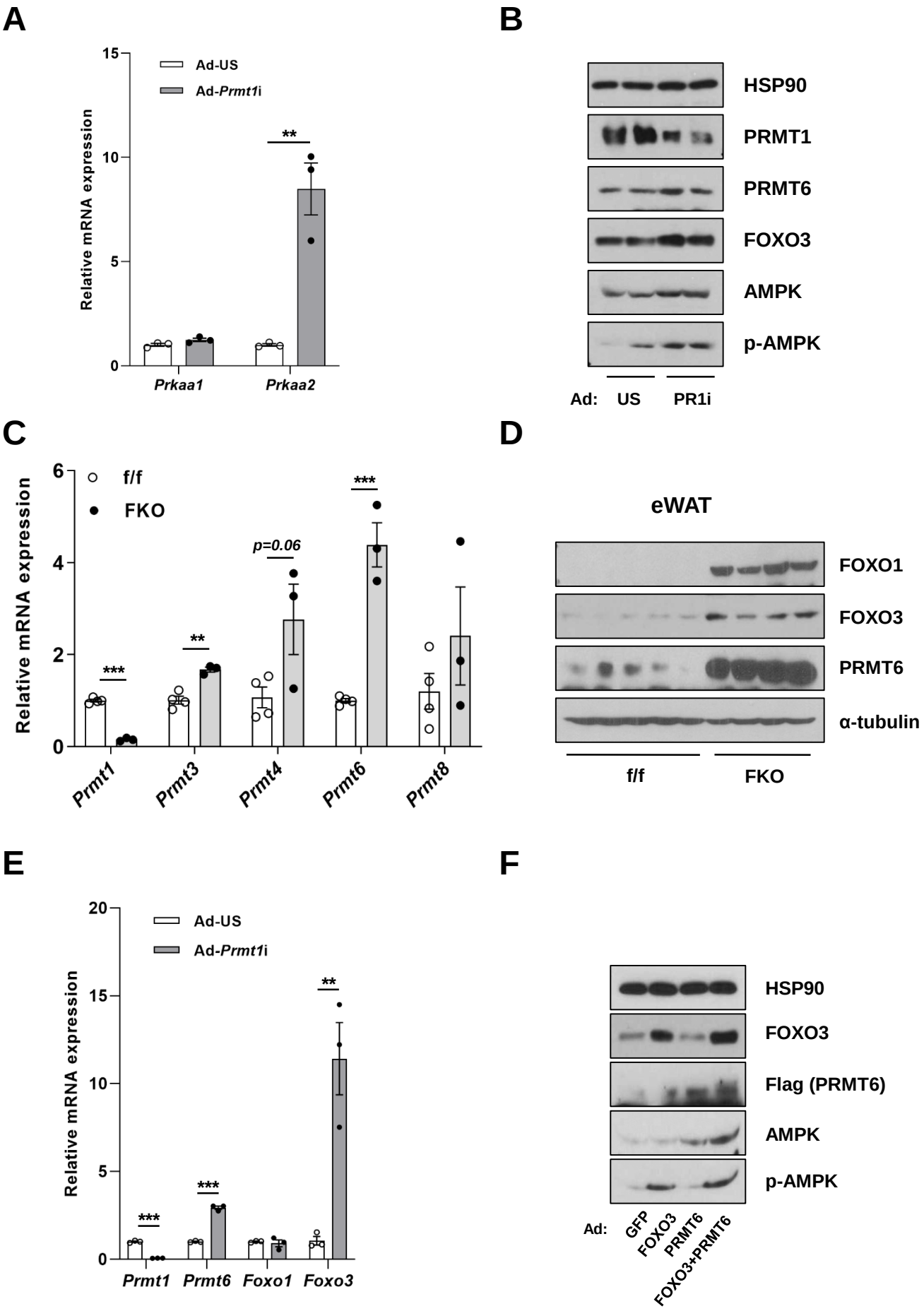

Supplementary Fig. 7

A

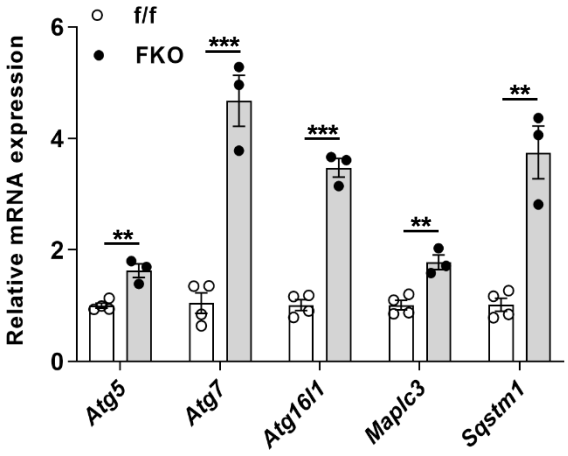

B

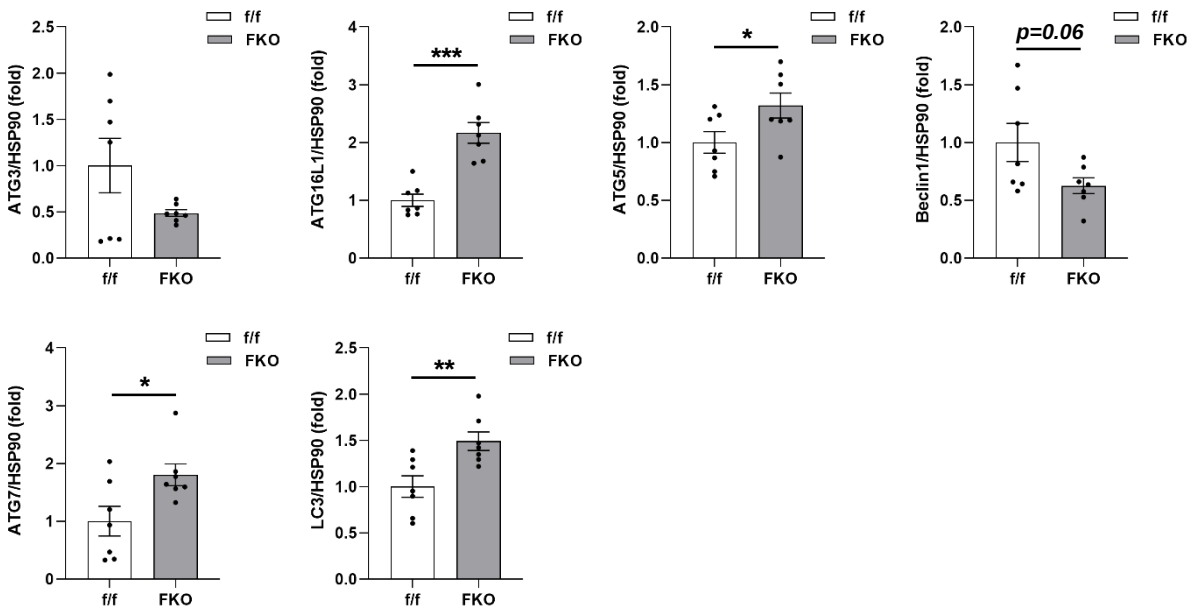

Supplementary Fig. 8

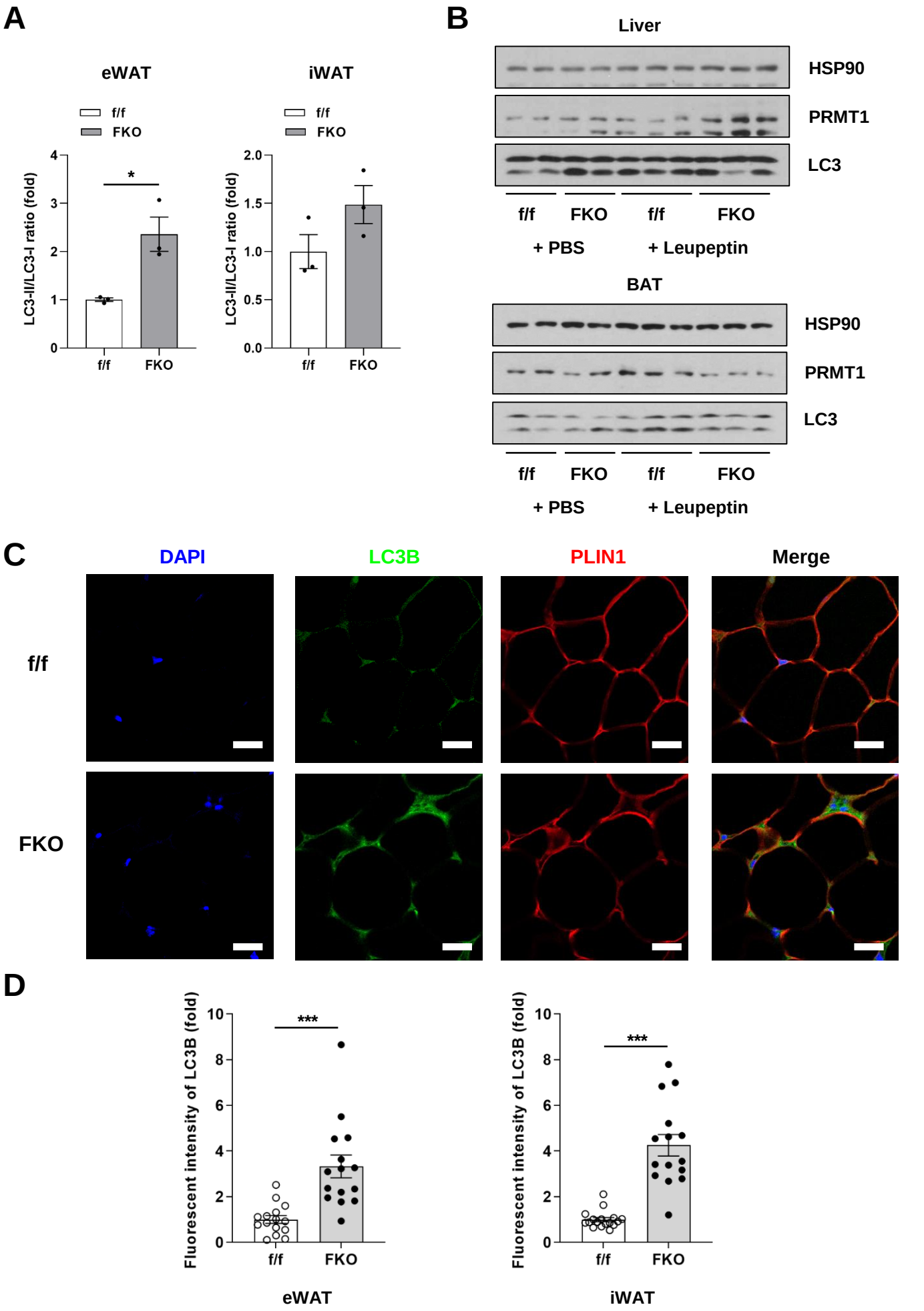

Supplementary Fig. 9

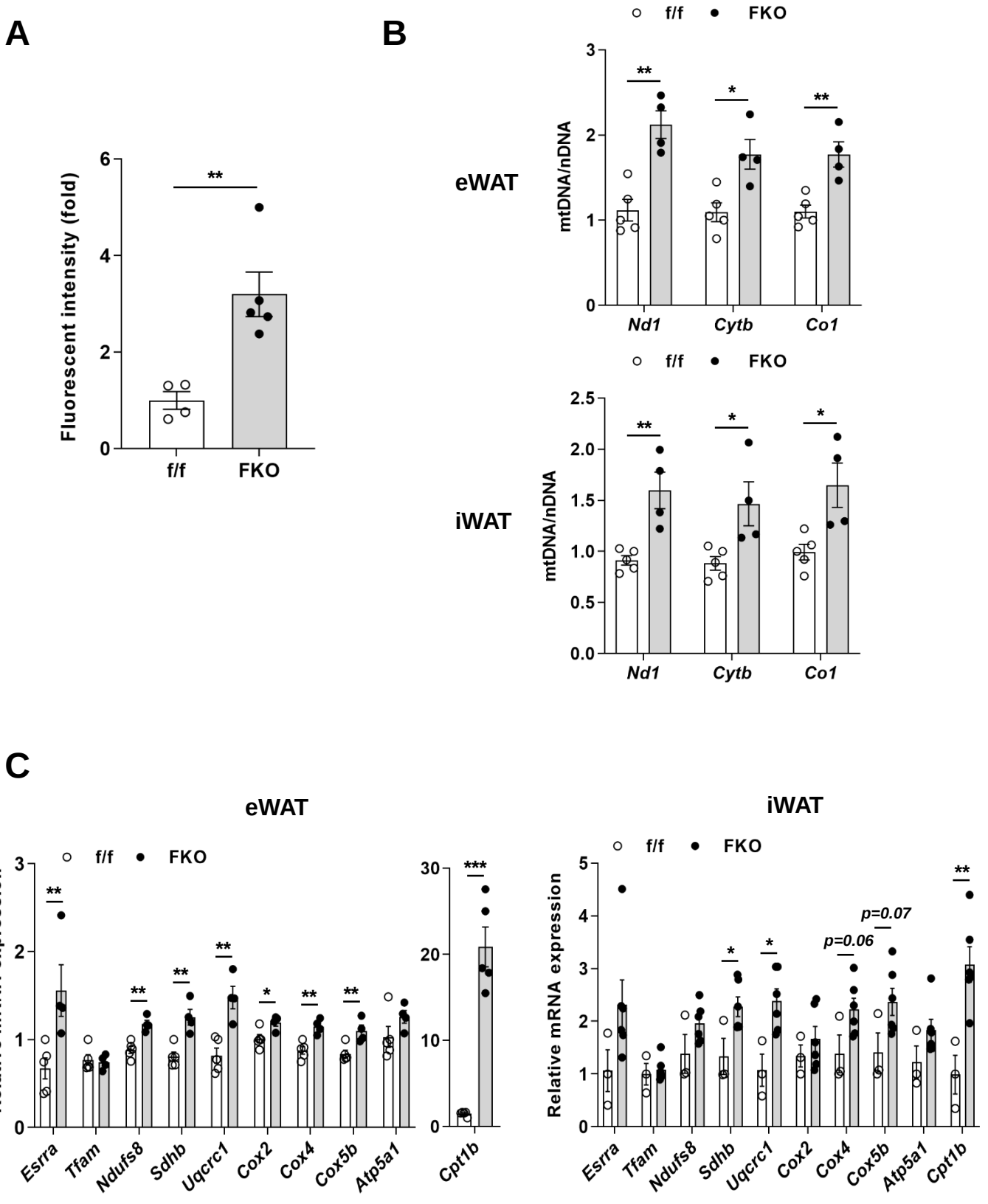

Supplementary Fig. 10

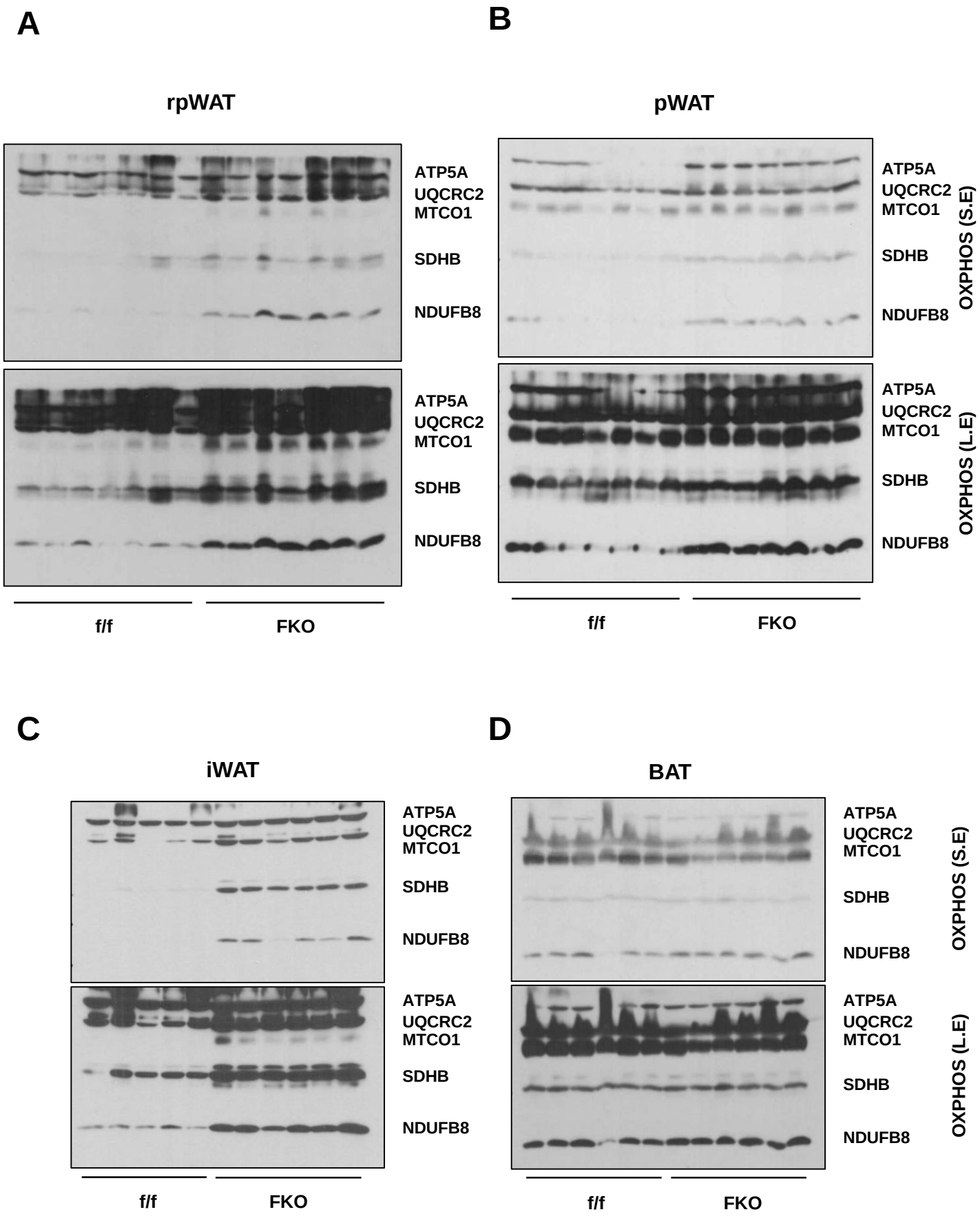

Supplementary Fig. 11

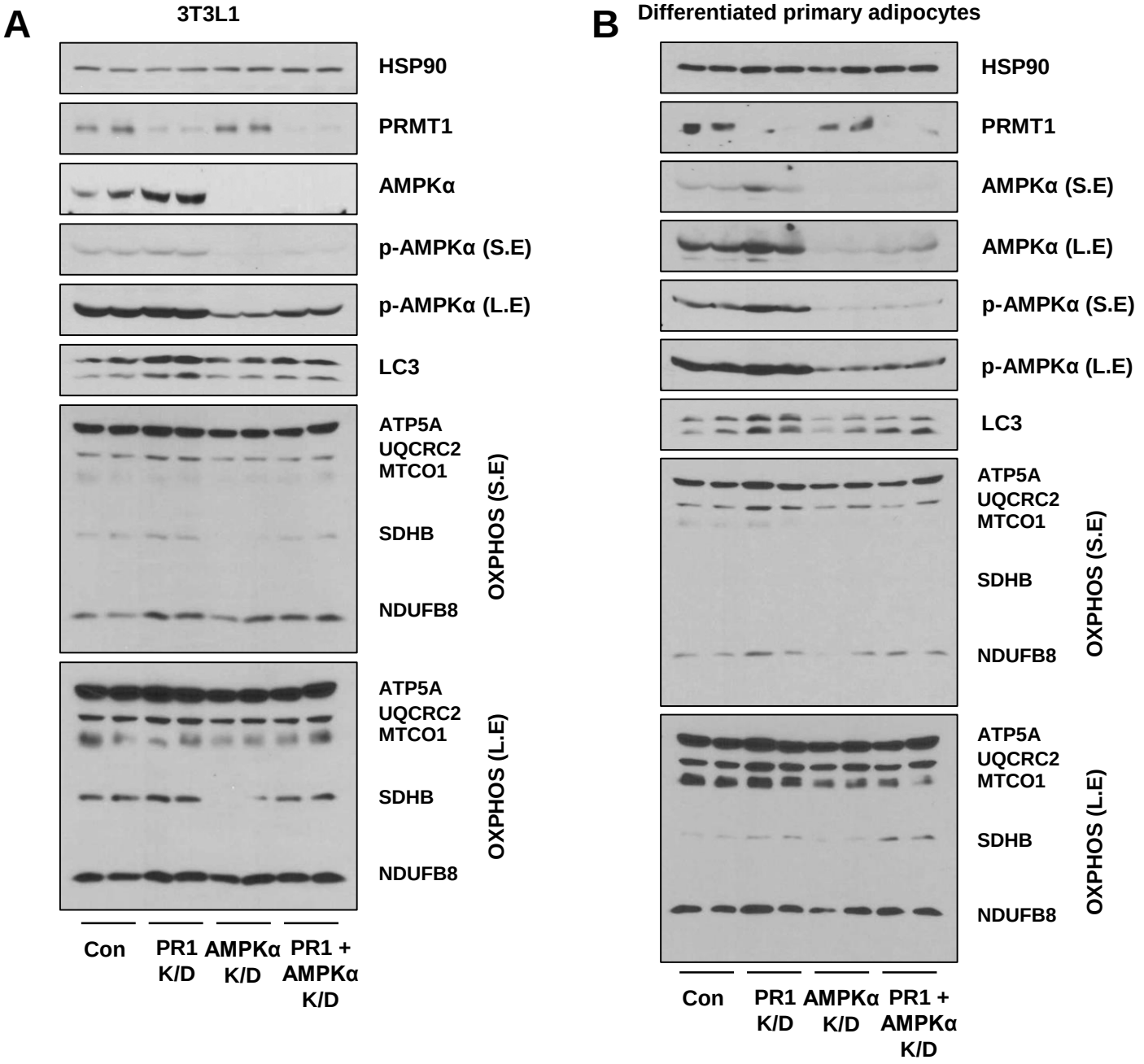

Supplementary Fig. 12

A

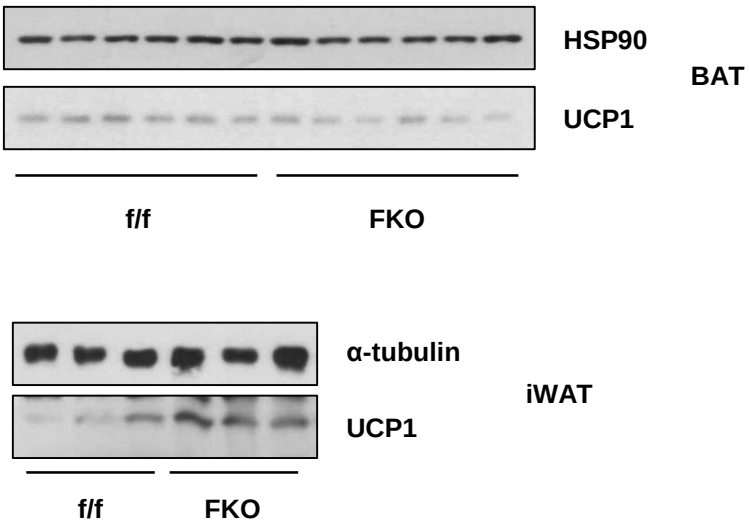

B

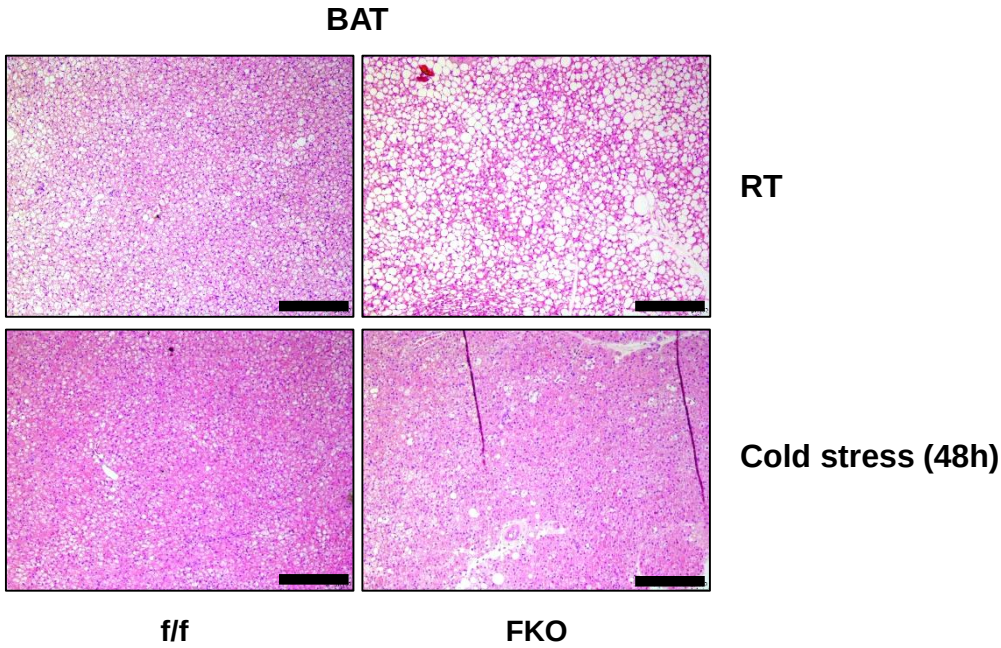

Supplementary Fig. 13

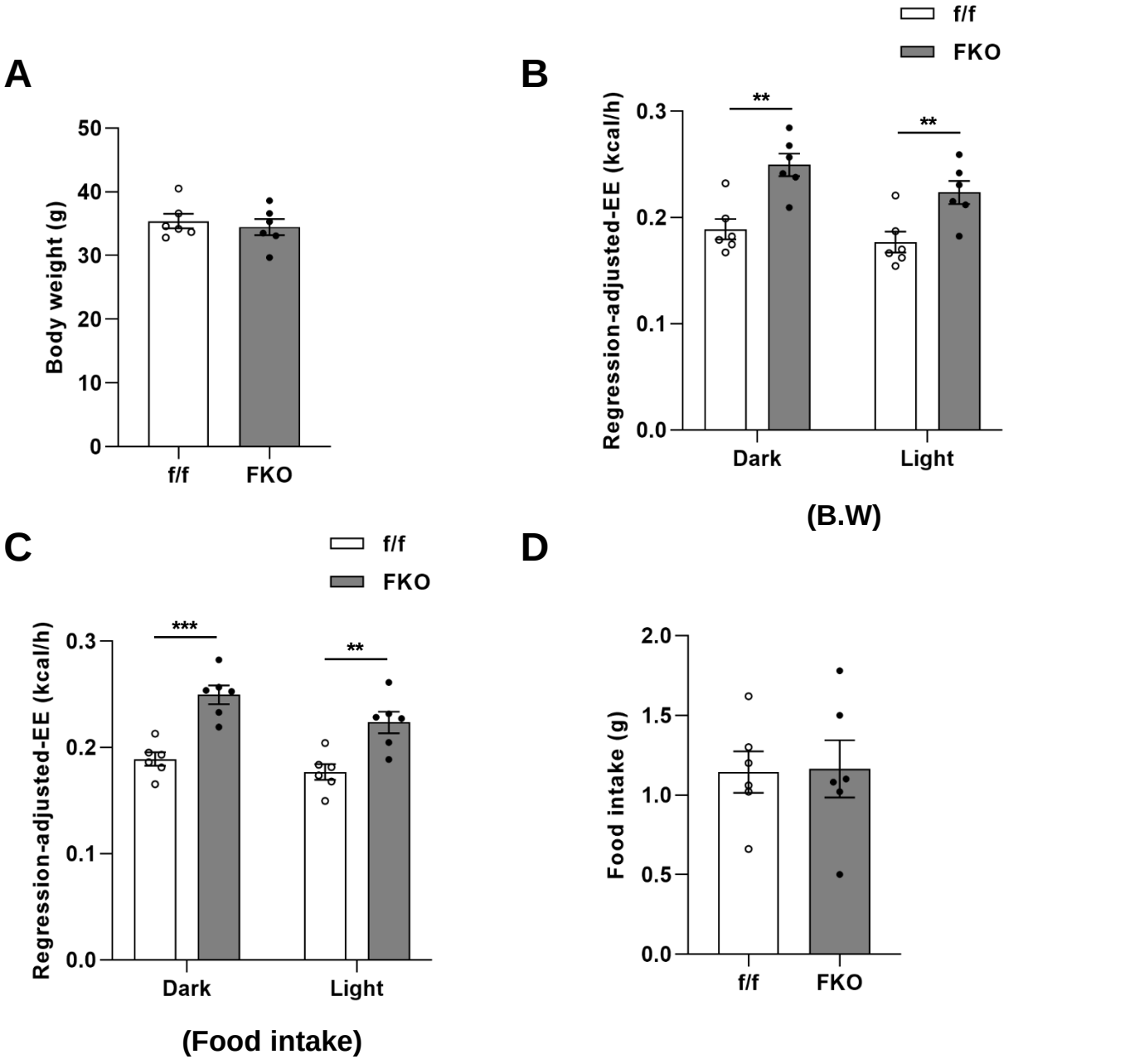

Supplementary Fig. 14

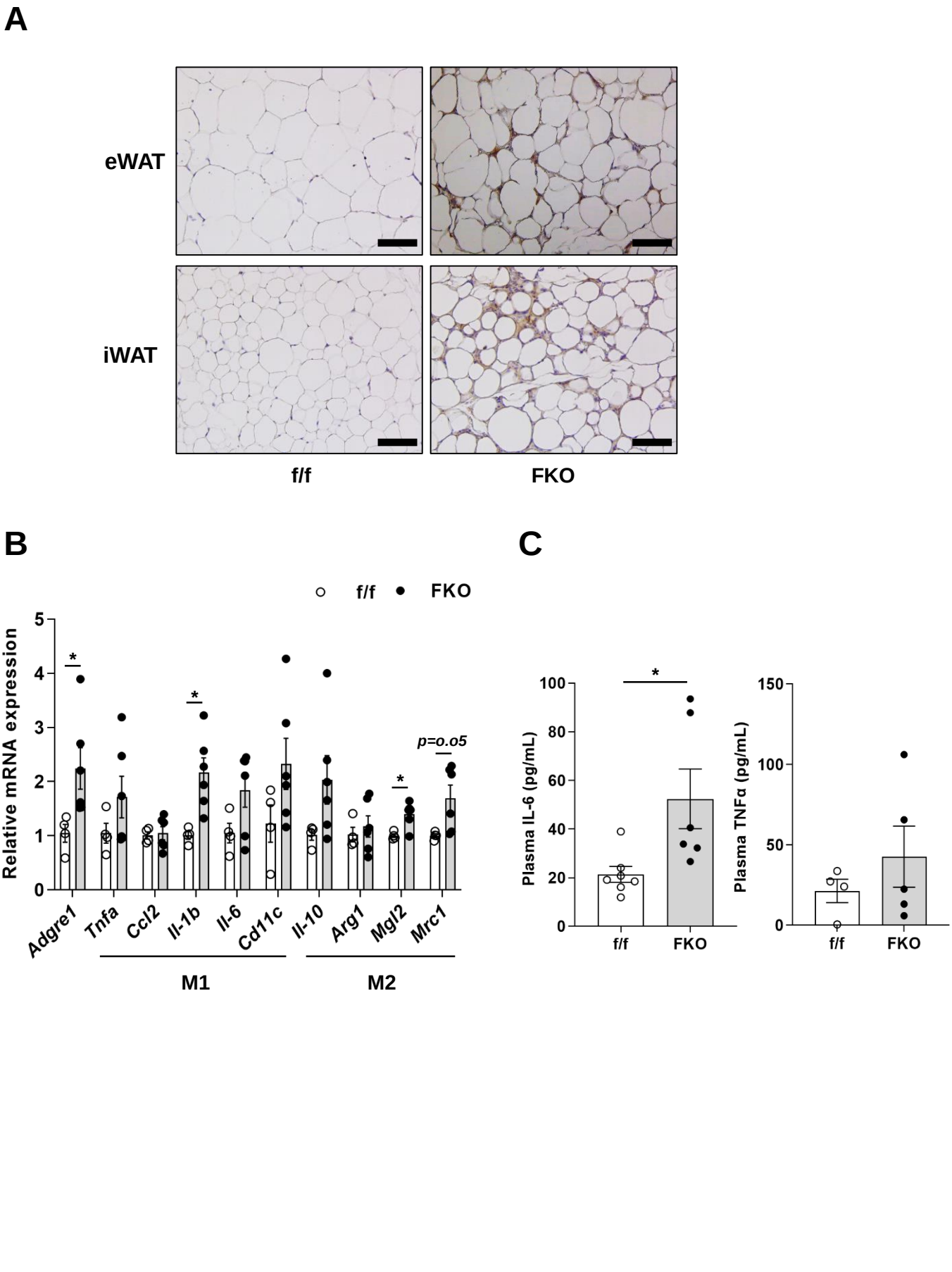

Supplementary Fig. 15

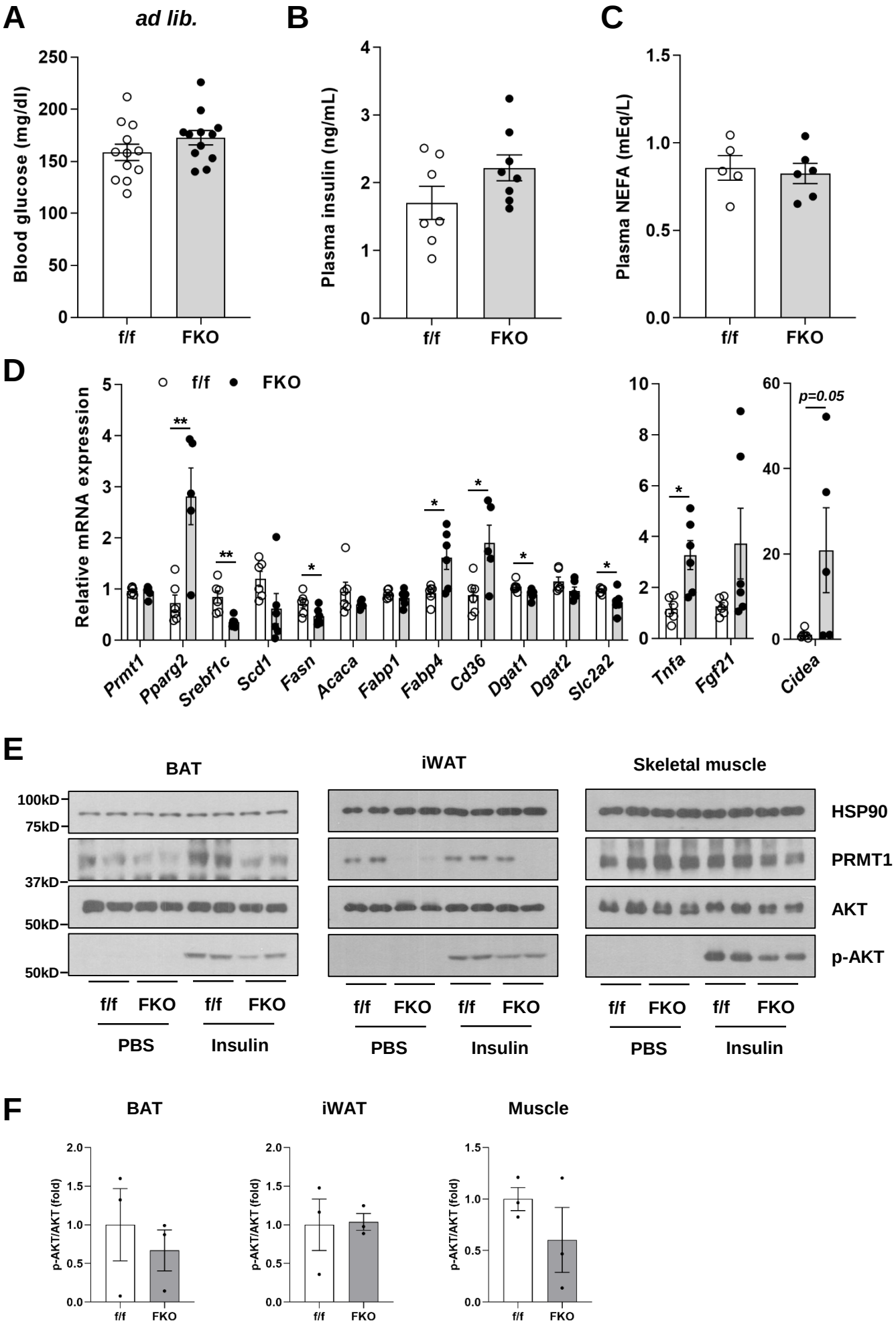

Supplementary Fig. 16